Application of Al/PI Composite Bumps to COG Bonding Process

Jen-Huang Jeng and T. E. Hsieh

***Abstract*—This work demonstrates the probing, testability and applicability of Al/PI (aluminum/polyimide) composite bumps to the chip-on-glass (COG) bonding process for liquid crystal display (LCD) driver chip packaging. The experimental results showed that the thickness of Al overlayer on PI core of the bump, the location of pin contact, and the bump configuration affect bump probing testability. The bump with type IV configuration prepared in this work exhibited excellent probing testability when its Al overlayer thickness exceeded 0.8 μm. We further employed Taguchi method to identify the optimum COG bonding parameters for the Al/PI composite bump. The four bonding parameters, bonding temperature, bonding time, bonding pressure and thickness of Al overlayer are identified as 180 °C, 10 s, 800 kgf/cm^2 and 1.4 μm, respectively. The optimum bonding condition was applied to subsequent COG bonding experiments on glass substrates containing Al pads or indium tin oxide (ITO) pads. From the results of resistance measurement along with a series of reliability tests, Al pad is found to be good substrate bonding pad for Al/PI bump to COG process. Excellent contact quality was observed when the bumps had Al overlayer thickness over 1.1 μm. As to the COG specimens with substrate containing ITO pads, high joint resistance suggested that further contact quality refinement is necessary to realize their application to COG process.**

***Index Terms*—Al/PI composite bumps, bonding, COG process, probing testability, reliability tests.**

I. INTRODUCTION

THE packaging of driver chips is one of the key technologies involved in the assembly of liquid crystal display (LCD) modules. In the LCD packaging, assembly technologies such as surface mount technology (SMT), tape automated bonding (TAB) and chip-on-glass (COG) process have been utilized. Among these, the COG process is the most favorable technology due to its capability of miniaturization, low cost, high density, high reliability, and ease of repair [1]. In COG process, the bonding of driver chips to the substrate can be achieved by using metal bonding [2], resin bonding [3], [4], conductive paste bonding [5], [6], and conductive particle bonding [7], [8]. Except for metal bonding, it is always necessary to deposit joint bumps on the bonding pad of driver chip. Gold (Au) is the material most commonly seen in wafer bumping [9], [10]. However, the fabrication of Au bump is rather complicated and it must be processed in an area separated from IC manufacturing to avoid Au contamination [11]. The complication increases not only the production cost but also the possibility of IC damage through shipping and handling. In addition, careful control of the hardness of Au bumps is vital. If the bumps have nonuniform hardness, they will deform unevenly during bonding and a satisfactory contact quality is difficult to obtain. Furthermore, if the bumps have nonuniform height or the bonding equipment has misaligned planarity, harder bumps will exert excessive force on the driver chip and cause damage to the active area under the bonding pads.

In order to remedy the deficiencies of Au bump, the polymer-cored bump coated with thin conductive layer was hence developed [10], [12]. Nishimori et al., for instance, employed photosensitive polyimide (PI) to form the core of bumps of large aspect ratios [12]. Their bumps exhibited excellent height uniformity and mechanical properties for chip bonding and, with appropriate bump-surface metallization, subsequent solder bond could be easily achieved.

This purpose of this work is to study the applicability of Al/PI composite bumps for the COG bonding process. We first prepared Al/PI bumps with different geometrical configurations and evaluated their probing testability. There are two square bumps with different sizes of top surface, a bump with a strip-like shape, and a bump containing two individual bumps on a bonding pad. The bumps exhibiting satisfactory probing testability were adopted in subsequent COG experiment.

There are two major types of bonding pad materials for LCD panels: indium tin oxide (ITO) and metal thin film. ITO is the common pad material for driver IC chip in twist neumatic (TN) and super twist neumatic (STN) types LCD panels. Metallic thin films such as aluminum (Al) and chromium (Cr) are used for thin-film-transistor (TFT) LCD panel. In COG experiment, we prepared the glass substrates containing Al pads or ITO pads to bond with Al/PI composite bumps on the chip. We identified the optimum bonding conditions of COG process using Taguchi method and evaluated the contact quality of joints by resistance measurement and a series of reliability tests.

II. EXPERMENTAL

A. Preparation of Bumped Chips

Dummy chips containing Al/PI composite bumps were used for the probing test, COG bonding parameter characterization, and reliability tests. Fig. 1 illustrates the preparation procedure of bumped chips.

A 0.5 μm thick Al layer was first deposited onto the 4-in Si wafer using a CVC 610 sputter system. The Al layer was then patterned to form the base conductive layer of the bumps.

Manuscript received June 1, 2000; revised February 8, 2001. This work was recommended for publication by Associate Editor R. Chanchani upon evaluation of the reviewers' comments. This work was supported in part by the National Science Council, R.O.C., under Contract NSC 89-2216-E009-018.

J.-H. Jeng is with the Microview Technology Corporation, Taoyuan, Taiwan, R.O.C.

T. E. Hsieh is with the Department of Materials Science and Engineering, National Chiao Tung University, Hsinchu, Taiwan, R.O.C.

Publisher Item Identifier S 1521-3331(01)04785-7.

1521–3331/01$10.00 © 2001 IEEE

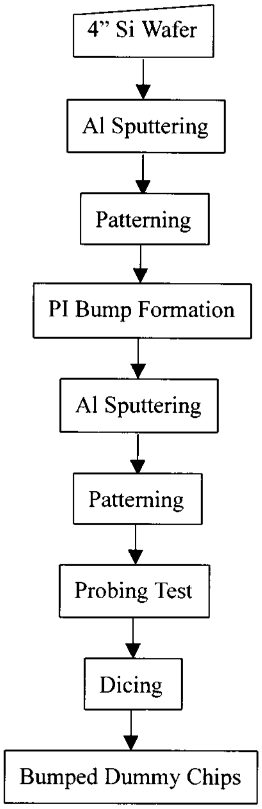

Fig. 1. Flowchart of bumped chip preparation.

Next, the core of composite bumps was formed using OCG 514 PI by Olin/Ciba-Geigy through a series of processes, namely, spin coating, soft baking, curing, and photolithography. Fig. 2 illustrates the procedure to form PI bumps with 15 μm height. Another Al layer was then sputtered on the top of PI core and patterned into desired structures. The thickness of this Al overlayer might affect the bonding character, so it was taken as one of the variables for subsequent optimum COG bonding parameter characterization. The Al overlayer thickness deposited was 0.2 μm, 0.5 μm, 0.8 μm, 1.1 μm, 1.4 μm, 1.7 μm, or 2.0 μm. We prepared Al/PI bumps of different configurations as shown in Fig. 3(a) to (d). They are assigned as type I, type II, type III, and type IV bumps accordingly. The top surface area of types I and II square bumps are 20 μm $\times$ 20 μm and 50 μm $\times$ 50 μm, respectively. The type III bump was designed for fine-pitch COG bonding and prepared by eliminating the etching of sidewall in between the neighboring PI cores. It has a strip-like top surface with the area of 90 μm $\times$ 20 μm. Type IV bump comprises two individual bumps separated by a distance of 40 μm on a bonding pad and each bump owns the top surface area of 50 μm $\times$ 20 μm. All types of Al/PI bumps were grown along the two long sides of the chip and each array contained 66 bumps.

B. Probing Test

Prior to COG bonding, all types of bumps was sent to a self-designed probing utility incorporating with a current-voltage tester to evaluate their probing testability. Electrical connection between the tester and the bumped chip was *via* a probing card containing 36 tungsten-rhenium (W-Re) probing pins. The pin had a round flat tip head with diameter about 10 μm. During the test, the probing pins simply touched on the bumps without scrubbing or ultrasonic motion. The bumps exhibiting unacceptable contact resistance (greater than 1 Ω or the voltage reading over 40 mV at a constant input current of 40 mA) were rated to fail the probing test.

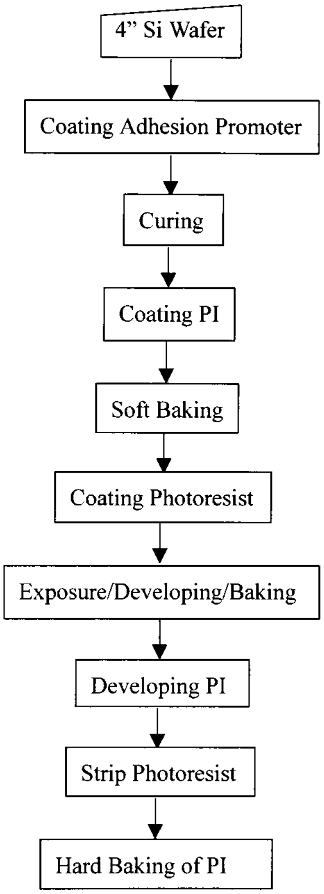

Fig. 2. Procedure of PI bump preparation.

C. Preparation of Glass Substrates

The substrate was 300 mm $\times$ 300 mm, single-side polished Corning glass for LCD panel. It was first deposited either with a metal layer consisted of 0.05 μm thick Cr and 0.6 μm thick Al or with a 0.1 μm thick ITO layer. After deposition, the deposited layer was patterned to form the bonding pads. The glass was then cut to appropriate size for subsequent COG bonding.

D. Characterization of COG Bonding Parameters

The previously prepared bumped chips were bonded to the glass substrate already coated with Sony 7130IQ anisotropic conductive film (ACF) by a self-designed COG bonder. The Sony 7130IQ ACF is comprised of epoxy matrix filled with gold-plated polymer balls. There is an additional insulating layer over the gold-plated ball, which was cracked during subsequent thermocompression process to achieve electrical conduction between the bumps and bonding pad. The bonding parameters were varied and their values are as follows: bonding temperature (180 °C, 200 °C, 220 °C); bonding time (5 s, 10 s, 15 s); bonding pressure (400 kgf/cm^2, 600 kgf/cm^2, 800 kgf/cm^2); thickness of Al overlayer (0.2 μm, 0.8 μm, 1.4

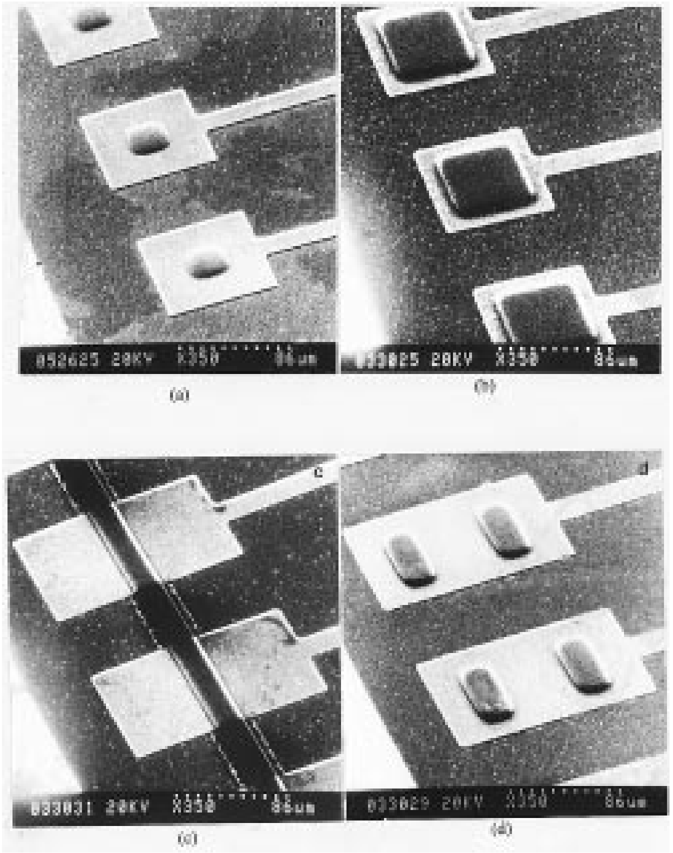

Fig. 3. Configuration of Al/PI composite bumps: (a) type I, (b) type II, (c) type III, and (d) type IV.

μm). The contact resistance of each bump joint was measured immediately after bonding. The COG specimens were subsequently stored in a 60 °C/90%RH ambient for 100 hours and the resistance of bump joints was measured again. All the resistance data were analyzed by the Taguchi method and, through an identification test, the optimum bonding parameters were obtained.

E. Reliability Tests

The untested type III bumped chips and the probe tested type IV bumped chips with various Al overlayers thickness were selected to form the COG specimens according to the optimum bonding condition determined previously. After the resistance of the bump joints was measured, the specimens were sent to four distinct types of reliability tests including a 60 °C/90%RH storage test, a 85 °C storage test, a -20 °C storage test, and a -25 °C to 70 °C thermal cycle test. For thermal cycle test, the dwell time at low and high temperatures was 30 min, while the transition time between low and high temperatures was 1 min. Several COG specimens utilizing type IV bumps were further encapsulated with silicone resin and sent to the 60 °C/90%RH test.

The reliability of the bump joint was evaluated in terms of the resistance change of the specimens measured after different storage times/cycles of the tests. For each type of reliability tests, twenty COG specimens were evaluated.

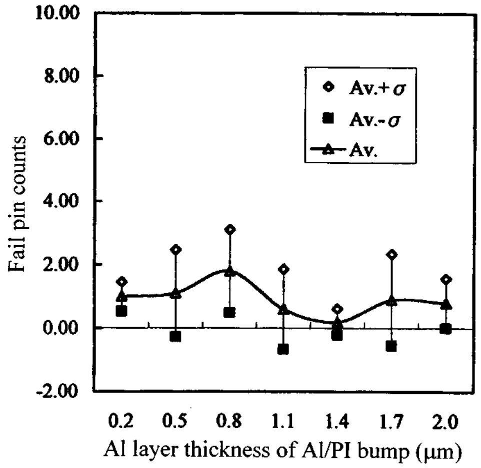

Fig. 4. Probing test results for type I Al/PI bump.

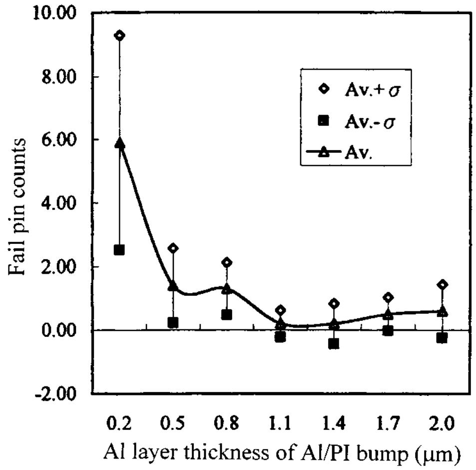

Fig. 5. Probing test results for type II Al/PI bump.

III. RESULTS AND DISCUSSION

A. Probing Test

The probing test results for the four different types of Al/PI bumps are shown in Figs. 4 to 7. In these figures, the ordinate is the fail pin counts (i.e., the number of pins exhibiting unacceptable contact resistance over 1 Ω in probing test) while the abscissa is the thickness of Al overlayer. For Al/PI bump with type I configuration, it exhibits unstable probing testability regardless of the increasing of Al overlayer thickness up to 2.0 μm, as shown in Fig. 4. For types II, III and IV Al/PI bumps, the average fail pin counts and its standard deviation decrease with increasing Al overlayer thickness, as shown in Figs. 5 to 7. For type IV Al/PI bump, as shown in Fig. 7, both average fail pin counts and standard deviation converge to zero when the thickness of Al overlayer exceeds 0.8 μm. This indicates that an Al/PI bump has excellent probing testability when the Al overlayer is thick enough to sustain the puncture action of probing. However, as shown in Figs. 5 and 6, unstable probing testability still appears in types II and III Al/PI bumps.

The irregular testability observed in type I Al/PI bump is attributed to the relatively small top surface area of the bump that

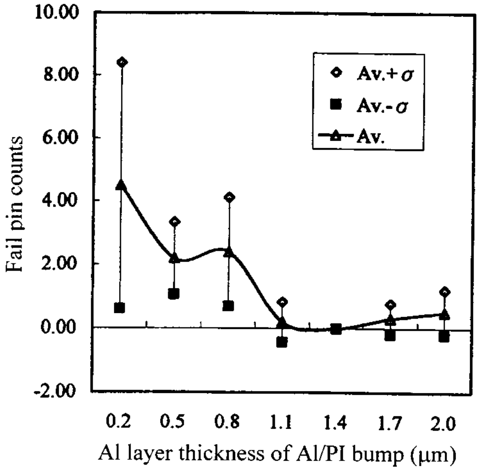

Fig. 6. Probing test results for type III Al/PI bump.

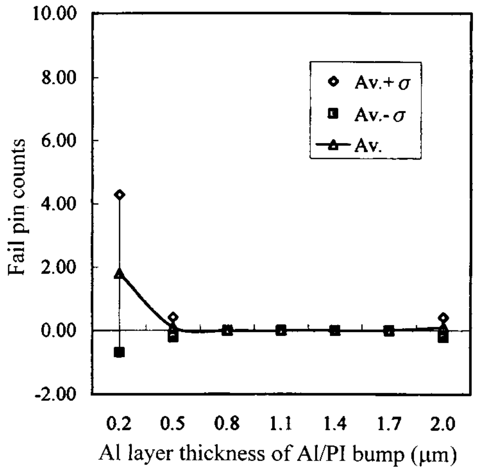

Fig. 7. Probing test results for the type IV Al/PI bump.

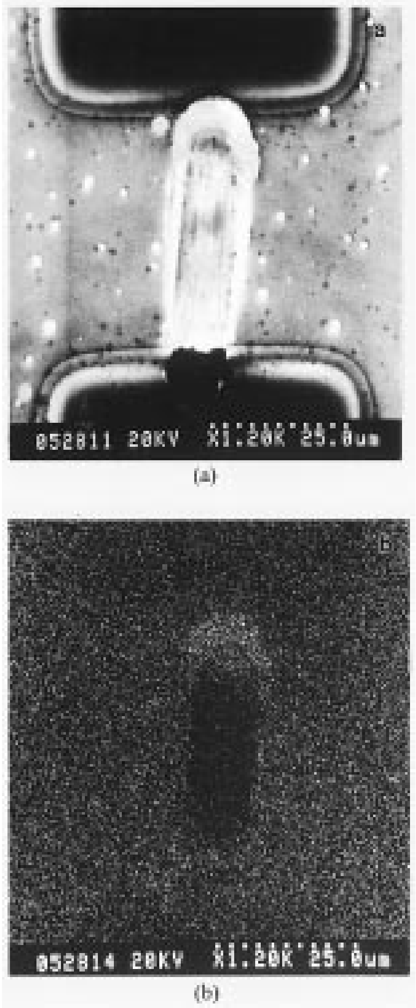

Fig. 8. (a) Surface morphology of the tested type IV bump with Al overlayer thickness $= 0.2$ μm and (b) Al element mapping of (a).

causes inconsistent contact between the probing pins and the bumps. Though the types II and III Al/PI bumps have larger top surface area assuring good contact between the probing pins and bumps, irregular probe testability is still observed, as shown in Figs. 5 and 6. It is known that the probing pins must possess appropriate hardness and sharpness to penetrate the oxide layer on Al (about 3 nm at room temperature [13]) so as to establishes the electrical conduction. However, the probing pins should not punch through the Al overlayer to reach the PI core of the bumps. Otherwise, the insulating nature of PI would inhibit electrical contact and cause the test failure. In the testing of types II and III Al/PI bumps, Al overlayer punch-through might be resulted from the elastic softness of PI core and inappropriate probing force. Undiminished fail pin counts were hence observed in the test results of these two types of bumps.

During the probing test of type IV bumps, we placed the probing tip on the area in between the two individual bumps instead of on the top surface of the bumps. Figs. 8 to 10 show the SEM (scanning electron microscope) images of the surface morphologies and Al element mappings of the tested bumps with Al overlayer thickness of 0.2 μm, 0.5 μm and 0.8 μm, respectively. As revealed by the Al element mappings shown in Figs. 8(b), 9(b) and 10(b), no punch-through in Al overlayer when its thickness is equal to 0.8 μm. When the thickness of Al overlayer exceeds such a threshold value, type IV Al/PI bump exhibits excellent testability, as shown in Fig. 7. The results above also indicate that for Al/PI composite bumps the testing probe should be placed on the area where hard substance such as Si is the substrate of Al layer to achieve satisfactory testability.

Probing test of the four types of Al/PI composite bumps indicates that in addition to the thickness of Al overlayer, the geometry and configuration of composite bumps are also important factors for the probing testability. Appropriate design of bump structure is thus vital in realizing the applications of the Al/PI composite bumps.

B. Characterization of COG Bonding Parameters

The optimum COG bonding parameters were characterized by the Taguchi method with an L9(3^4) table (see Table I). Using the formula derived from the Taguchi's theory, we calculated $\Delta R_{\rm av}$ (average contact resistance change) and S/N ratio (signal to noise ratio) for each set of experiments listed in Table I. Since the optimum COG bonding conditions could be determined by analyzing the variation of S/N ratio, the response of S/N ratio

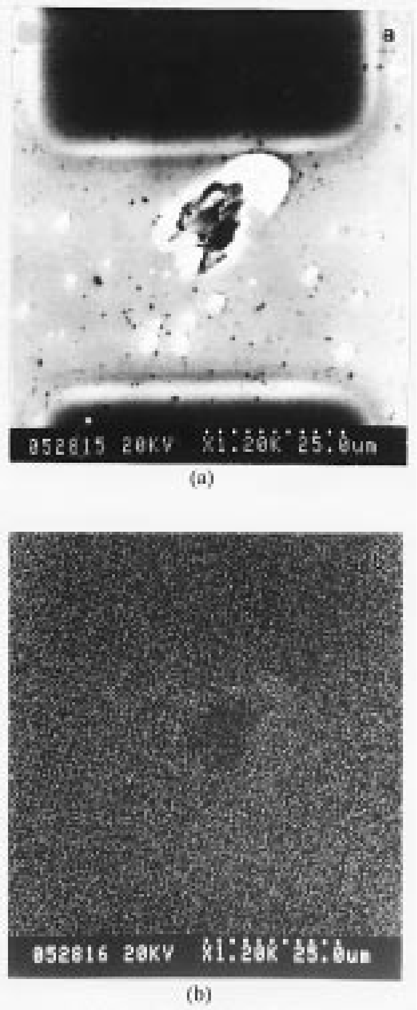

Fig. 9. (a) Surface morphology of the tested type IV bump with Al overlayer thickness $= 0.5\ \mu$m and (b) Al element mapping of (a).

for each value of bonding parameters were also calculated and the results were plotted in Fig. 11. It reveals that bonding pressure is the most significant factor affecting the S/N ratio while bonding temperature plays only a minor role. Fig. 11 also indicates that the optimum COG bonding parameters are the combination of $A_1B_2C_3D_3$, that is, 180 °C, 10 s, 800 kgf/cm^2 and 1.4 μm for bonding temperature, bonding time, bonding pressure and thickness of Al overlayer respectively. Subsequent identification experiment showed that the variation of contact resistance of bump joints was no more than 2.3 Ω. This evidences that at such a bonding condition the Al/PI composite bumps are able to form joints with very stable contact quality.

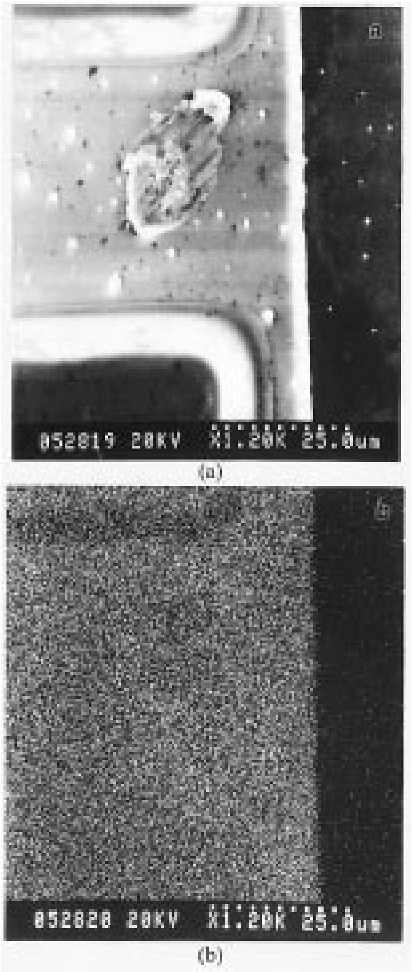

Fig. 10. (a) Surface morphology of the tested type IV bump with Al overlayer thickness $= 0.8\ \mu$m and (b) Al element mapping of (a).

TABLE I
BONDING PARAMETERS, ΔR_{av}, AND S/N RATIO FOR EACH SET OF EXPERIMENT

Factor / Exp.	Temperature (°C)	Time (sec)	Pressure (kgf/cm^2)	Al Thickness (μm)	ΔR_{av} (Ω)	S/N Ratio
1	A_1	B_1	C_1	D_1	48.0	-37.26
2	A_1	B_2	C_2	D_2	1.5	-6.24
3	A_1	B_3	C_3	D_3	0.9	-2.0
4	A_2	B_1	C_2	D_3	2.6	-12.66
5	A_2	B_2	C_3	D_1	1.3	-5.89
6	A_2	B_3	C_1	D_2	25.3	-34.51
7	A_3	B_1	C_3	D_2	1.5	-8.21
8	A_3	B_2	C_1	D_3	5.1	-19.58
9	A_3	B_3	C_2	D_1	7.4	-23.51

A_1 = 180°C; A_2 = 200°C; A_3 = 220°C.
B_1 = 5 sec; B_2 = 10 sec; B_3 = 15 sec.
C_1 = 400 kgf/cm^2; C_2 = 600 kgf/cm^2; C_3 = 800 kgf/cm^2.
D_1 = 0.2 μm; D_2 = 0.8 μm; D_3 = 1.4 μm.

C. COG Bonding Experiment

Fig. 12 shows the contact resistance of COG specimen fabricated by chips containing type IV bumps and Al pads on glass substrate. The average resistance is in the range of 5 to 10 Ω and both the resistance and its σ (standard deviation) decreases with increasing Al overlayer thickness. When the thickness of Al overlayer exceeds 1.1 μm, the average resistance is about 5 Ω and $\sigma < 1\ \Omega$. Fig. 13 gives the contact resistance of COG specimen using ITO pads. Even though the convergence of contact resistance and σ is observed, the average resistance of COG specimens using ITO pads is clearly higher than the specimens using Al pads. The resistance is about 80 Ω and $\sigma < 40\ \Omega$ when the thickness of Al overlayer is equal to 1.1 μm. This might be caused by the rough surface of ITO pads, which inhibited good contact between the bumps and the pads.

The electrical properties of COG specimen containing type III Al/PI bumps were also evaluated. Fig. 14 shows the variation

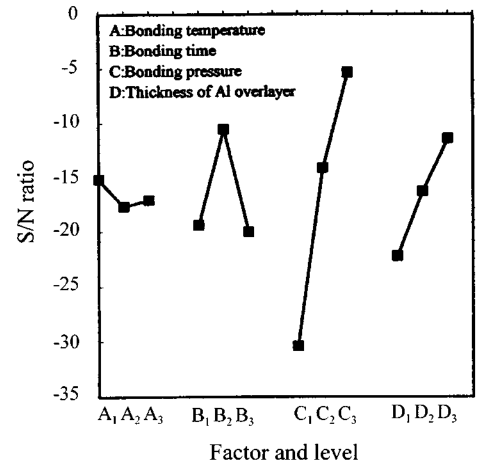

Fig. 11. Response of S/N ratio to each of the COG bonding parameters.

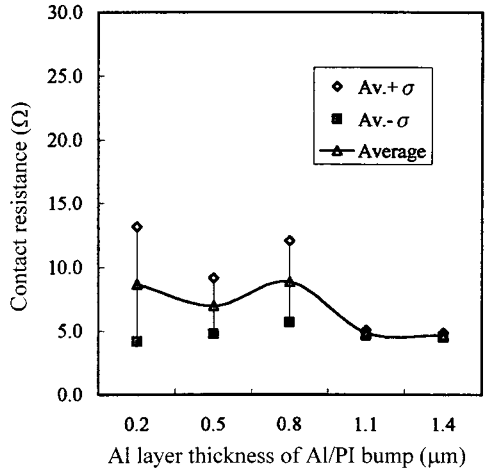

Fig. 12. Contact resistance of COG specimen fabricated by bonding the chips containing type IV bumps on glass substrate with Al pads.

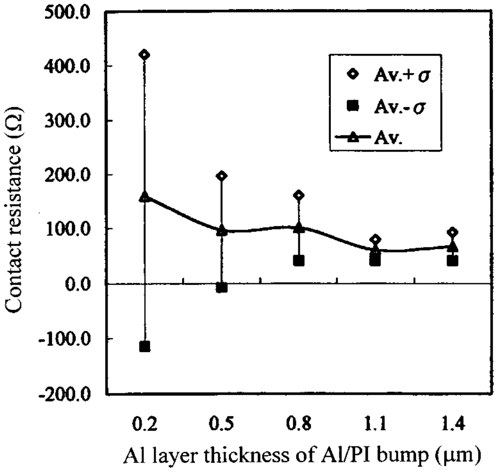

Fig. 13. Contact resistance of COG specimen fabricated by bonding the chips containing type IV bumps on glass substrate with ITO pads.

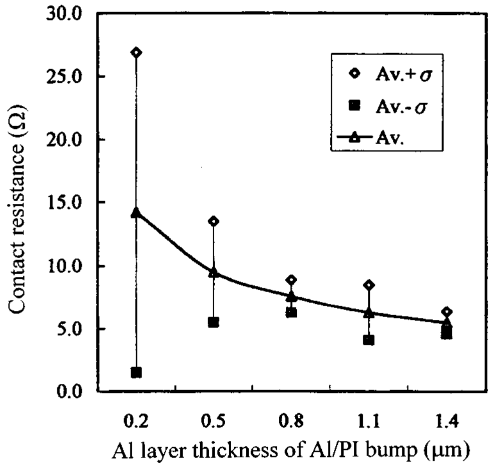

Fig. 14. Contact resistance of COG specimen fabricated by bonding the chips containing type III bumps and on glass substrate with Al pads.

of contact resistance as a function of Al overlayer thickness for type III bumps bonded on Al pads of glass substrate. We again observe the decreasing trend of contact resistance and σ with the increasing of Al overlayer thickness. The average resistance is less than 10 Ω and $\sigma < 3\ \Omega$ when Al overlayer thickness is greater than 1.1 μm. Compared with the test results of COG specimen using type IV bumps, the contact resistance is only slightly higher for the specimen using type III bumps. One possible cause of this result might be that the smaller top surface area of the type III bump reduces the number of conductive particles available in between the bump and bonding pad. Nevertheless, it did exhibit satisfactory contact quality. By combining the design concepts of type III and IV bumps, it is possible to form a bump structure with excellent probe testability for COG bonding applications.

D. Reliability Tests

The chips containing untested type III bumps and probe tested type IV bumps were utilized to form the COG specimens for the reliability test. Type III bump was chosen because of their potential applications to fine-pitch bonding where as type IV Al/PI bump was chosen because of their excellent probing testability. These two types of Al/PI bumps of various Al overlayer thickness were bonded to the glass substrates padded with Al or ITO in accord with the optimum bonding conditions obtained above. Four different reliability tests described previously were performed and the contact resistances of the COG specimens subjected to these tests were then measured.

Figs. 15 to 18 illustrate $\Delta R_{\rm av}$ of the joints and the corresponding σ as a function of Al overlayer thickness for COG specimens fabricated with type IV bumps and the glass substrate with Al pads. It can be readily seen from all the reliability tests that the values of $\Delta R_{\rm av}$ and σ of the COG specimens decrease with increasing Al overlayer thickness. When the thickness of Al overlayer exceeds 1.1 μm, the COG specimens subjected to the 60 °C/90%RH storage test have $\Delta R_{\rm av} < 1.8\ \Omega$ and $\sigma < 2.2\ \Omega$ (see Fig. 15). For the specimens subjected to the 85 °C-storage test, we obtained $\Delta R_{\rm av} < 1.2\ \Omega$ and $\sigma < 1.0\ \Omega$ (see Fig. 16). As to the specimens subjected to the -20 °C storage test and the -25 °C to 70 °C thermal cycle test, both $\Delta R_{\rm av}$ and σ approach to zero ohm regardless of the thickness of Al overlayer of the bumps, as shown in Figs. 17 and 18. The results above also indicate that high temperature/high humidity storage test is the strictest in evaluating the reliability of

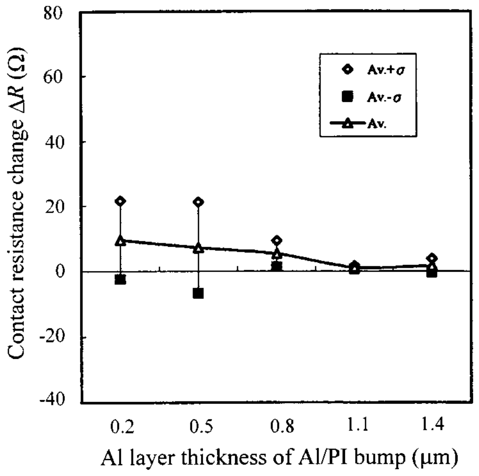

Fig. 15. Average contact resistance change of COG specimens subjected to 60 °C/ 90%RH storage test.

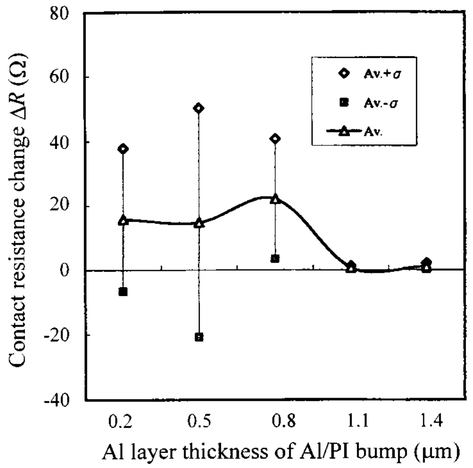

Fig. 16. Average contact resistance change of COG specimens subjected to 85 °C storage test.

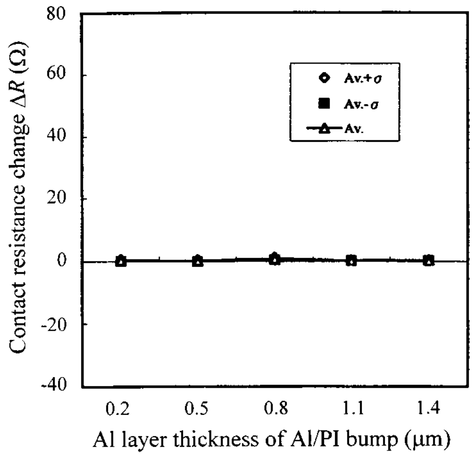

Fig. 17. Average contact resistance change of COG specimens subjected to −20 °C storage test.

COG specimens. Nevertheless, the specimens subjected to this test still possess excellent contact quality when the thickness of Al layer on PI core is greater than 1.1 μm.

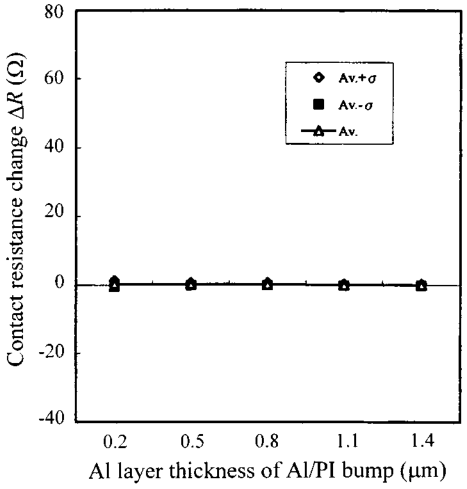

Fig. 18. Average contact resistance change of COG specimens subjected to −25 °C to 70 °C thermal cycle test.

TABLE II
AVERAGE VALUES OF ΔR_{av} and σ OF THE COG SPECIMENS SUBJECTED TO VARIOUS RELIABILITY TESTS

(Unit: ohms)

Sample type / Test type	Type III bumps				Type IV bumps			
	Al pads		ITO pads		Al pads		ITO pads	
	ΔR_{av}	σ	ΔR_{av}	σ	ΔR_{av}	σ	ΔR_{av}	σ
60°C/90%RH, 500 hr storage test	3.1	1.1	155.7	112.9	1.8	2.2	71.4	72.3
85°C, 500 hr storage test	7.7	7.6	219.4	233.1	1.2	1.0	198.8	291
-20°C, 500 hr storage test	-0.2	0.3	9.6	10.6	0.3	0.1	13.3	7.1
-25 to 70°C, 10 cycle thermal cycle test	0.1	0.3	-0.5	1.1	0.1	0.3	1.6	4.5

Table II summaries the values of ΔR_{av} and σ of all COG specimens subjected to various reliability tests. In these specimens, the Al layer on PI core was greater than 1.1 μm in thickness. For the COG specimens using Al pads on glass substrate, the maximum values of ΔR_{av} is 7.7 Ω and σ is 7.6 Ω. The satisfactory contact quality assures the applicability of Al/PI composite bumps in COG process with Al pads on glass. For the COG specimens bonded with ITO pads, both ΔR_{av} and σ were within of 200 Ω (see Table II for detail). Such resistance values are too high for practical applications and further work is required to improve the joint quality of COG specimen utilizing the Al/PI composite bumps and glass substrate with ITO pads.

For the COG specimens encapsulated with silicone resin, ΔR_{av} was 3.7 Ω and σ was 3.4 Ω for the specimens bonded with Al pads after a 500-h storage in 60°C/90%RH environment. As to the specimens bonded with ITO pads, ΔR_{av} was 176.5 Ω and σ was 153.6 Ω. It seemed encapsulation offered no substantial improvement on the contact quality of COG specimens prepared in this work.

IV. CONCLUSION

We have demonstrated the feasibility of Al/PI composite bumps to a COG bonding process for LCD driver IC. Among the four types of bumps prepared, excellent probing testability was achieved in type IV Al/PI composite bump with Al overlayer thickness exceeding 0.8 μm. The probing test indicated that the bump configuration and the thickness of Al overlayer were crucial to the probing testability of Al/PI composite bumps. Taguchi method was employed to characterize the optimum bonding parameters of Al/PI composite bumps applied to COG process. By analyzing the responses of S/N ratio to each of the bonding parameters and with the aid of identification experiment, the optimum bonding parameters were characterized as the following: bonding temperature $= 180\,^{\circ}\mathrm{C}$, bonding time $=$ 10 s, bonding pressure $= 800\ \mathrm{kgf/cm^2}$, and Al overlayer thickness $= 1.4\ \mu\mathrm{m}$. The COG bonding experiment was carried out according to the optimum bonding condition. In this part of the experiment, COG specimens were fabricated by bonding type III and type IV Al/PI composite bumps onto glass substrates containing Al pads or ITO pads. The interconnection resistance measurement revealed very good contact quality for both type III and type IV bumps bonded to glass substrate with Al pads. Four different types of reliability tests were performed on the COG specimens and the subsequent resistance measurement showed that good contact quality could be preserved for the bumps with Al overlayer thickness greater than 1.1 μm. This results indicate that, by combining the structure design of type III and IV bumps, an Al/PI composite bump with excellent probe testability can be formed for fine-pitch COG bonding applications. As to the COG specimens bonded with ITO pads, the interconnection resistance was found to be high and further refinements of contact quality are necessary to realize their applications to COG process.

ACKNOWLEDGMENT

The authors would like to thank Y.-C. Lee and S.-M. Chang, Electronics Research and Service Organization, Industrial Technology Research Institute (ERSO/ITRI), for their support of this work, and T.-H. Lin and M.-C. Tsai for their assistances on the specimen preparation and SEM characterization.

REFERENCES

[1] S.-M. Chang, “Packaging technology for liquid crystal display,” *Electron. Inform.*, pp. 14–18, Mar. 1995.

[2] M. Mori, Y. Kizaki, M. Saito, and A. Hongu, “A fine pitch COG technique for a TFT-LCD panel using an indium alloy,” *IEEE Trans., Comp., Hybrids, Manufact. Technol.*, vol. 16, pp. 852–857, Dec. 1993.

[3] K. Hatada, H. Fujimoto, T. Ochi, and Y. Ishida, “Applications of new assembly method: Micron bump bonding method,” in *Proc. IEEE CHMT’89 IEMT Symp.*, 1989, pp. 47–50.

[4] ——, “LED array modules by new technology microbump bonding method,” *IEEE Trans., Comp., Hybrids, Manufact. Technol.*, vol. 13, pp. 521–527, Sept. 1990.

[5] I. Katsuo, “Bump formation by using Ag-Pd paste for 356 pins LSI bonding in 15 seconds,” *Nikkei Microdevices*, pp. 49–51, July 1989.

[6] T. Tamura, I. Kobayashi, M. Uno, K. Adachi, M. Takeda, S. Hotta, Y. Bessho, and S. Nakamura, “A 2.8-in. point-defect-free a-Si TFT-LCD module for projection ED-TV assembled by a stud-bump-bonding COG method,” in *Proc. SID*, vol. 32, 1991, pp. 289–295.

[7] A. Nao, Y. Kounan, and F. Youco, “Anisotropic conductive film,” *Electron. Packag. Technol.*, vol. 8, no. 5, pp. 35–39, May 1992.

[8] F.-J. Wu, *Flip-Chip-on-Glass: Market, Material, Process Equipment for Flat Panel Display Industry, Part II: Flip-Chip-on-Glass Technology*. Taipei, Taiwan, R.O.C.: ERSO/ITRI, June 1996, pp. 3–36.

[9] T. S. Liu, W. R. R. de Miranda, and P. R. Zipperlin, “A review of wafer bumping for tape automated bonding,” *Solid State Technol.*, pp. 71–76, Mar. 1980.

[10] J. H. Lau, Ed., *Flip Chip Technologies*. New York: McGraw-Hill, 1996.

[11] J. C. C. Tsai, “Diffusion,” in *VLSI Technology*, 2nd ed, S. M. Sze, Ed. New York: McGraw-Hill, 1988, pp. 307–308.

[12] T. Nishimori, H. Yanagihara, K. Murayama, Y. Kama, and M. Nakamura, “Characteristics and potential application of polyimide-core-bump to flip chip,” *IEEE Trans., Comp., Hybrids, Manufact. Technol.*, vol. 19, p. 18, Mar. 1996.

[13] J. M. West, *Basic Corrosion and Oxidation*, Chichester, U.K.: Ellis Horwood, 1980, p. 167.

Jen-Huang Jeng received the M.S. degree from the Department of Materials Science and Engineering, National Chiao Tung University, Hsinchu, Taiwan, R.O.C., in 1996 and the B.S. degree in mechanical engineering from National Taiwan Institute of Technology, in 1987.

He had worked in Electronic Research and Service Organization (ERSO), Industrial Technology and Research Institute (ITRI), Taiwan, for over ten years as an Engineer involved in the process development relating to TAB and COG fabrications. Currently, he is the General Manager of Microview Technology Corporation in charge of the LCD module assembly.

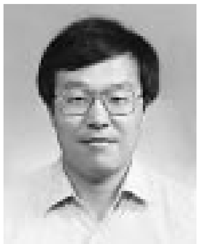

T. E. Hsieh received the B.S. degree in physics from National Taiwan Normal University, Taiwan, R.O.C., in 1979, the M.S. degree in materials science from National Tsing Hua University, Taiwan, in 1981, and the Ph.D. degree from the Massachusetts Institute of Technology, Cambridge, in 1988.

Currently, he is a faculty member with the Department of Materials Science and Engineering, National Chiao Tung University, Hsinchu, Taiwan. His research interests cover electronic packaging, storage media, thin-film technology, and materials characterization.